Bioinspired Design of Nanostructured Elastomers with Cross-Linked Soft Matrix Grafting on the Oriented Rigid Nanofibers To Mimic Mechanical Properties of Human Skin

Zhongkai Wang,[†] Feng Jiang,[†] Yaqiong Zhang,[†] Yezi You,[†] Zhigang Wang,[*,†] and Zhibin Guan[*,‡]

[†]CAS Key Laboratory of Soft Matter Chemistry, Department of Polymer Science and Engineering, Hefei National Laboratory for Physical Sciences at the Microscale, University of Science and Technology of China, Hefei, Anhui Province 230026, P.R. China and [‡]Department of Chemistry, University of California, 1102 Natural Sciences II, Irvine, California 92697-2025, United States

ABSTRACT Human skin exhibits highly nonlinear elastic properties that are essential to its physiological functions. It is soft at low strain but stiff at high strain, thereby protecting internal organs and tissues from mechanical trauma. However, to date, the development of materials to mimic the unique mechanical properties of human skin is still a great challenge. Here we report a bioinspired design of nanostructured elastomers combining two abundant plant-based biopolymers, stiff cellulose and elastic polyisoprene (natural rubber), to mimic the mechanical properties of human skin. The nanostructured elastomers show highly nonlinear mechanical properties closely mimicking that of human skin. Importantly, the mechanical properties of these nanostructured elastomers can be tuned by adjusting cellulose content, providing the opportunity to synthesize materials that mimic the mechanical properties of different types of skins. Given the simplicity, efficiency, and tunability, this design may provide a promising strategy for creating artificial skin for both general mechanical and biomedical applications.

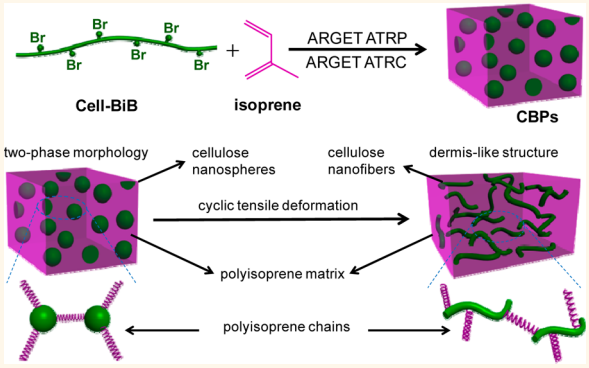

KEYWORDS: human skin · mechanical property mimicking · microphase separation · multiphase polymer · mechanical processing · nonlinear elasticity

Researchers have long been intrigued by the molecular mechanisms responsible for the nonlinear elasticity of soft biological tissues such as human skin.[1−3] Several examples have been reported in the design of nonlinear elastic materials to mimic biological systems including muscles,[4] sea cucumber dermis,[5] as well as spider silk.[6,7] Human skin has a three-layer structure: epidermis, dermis, and subcutaneous tissue.[8,9] Among these three layers, the dermis is the principal layer contributing to the mechanical properties of the skin.[10] The main structural components of dermis are collagen and elastin, two biopolymers with distinctively different mechanical properties. Semirigid collagen nanofibers provide the structural scaffold for dermis and are responsible for its strength.[11] Conversely, soft elastin fibers, intertwined with collagen fibers *via* covalent bonds, provide skin elasticity and resilience.[12] The chemical connectivity between collagen and elastin fibers prevents chain slippage and allows for skin to undergo large, reversible deformation. The unique combination of strong, semirigid collagen nanofibers and highly elastomeric elastin fibers chemically integrated in a two-phase nanocomposite gives rise to the nonlinear mechanical properties of human skin. For potential applications as skin substitutes and for tissue engineering, several skin-mimicking materials have been engineered to imitate various biological functionalities of human skin.[13−15] However, their

* Address correspondence to zgwang2@ustc.edu.cn, zguan@uci.edu.

Received for review August 12, 2014 and accepted December 26, 2014.

Published online December 31, 2014
10.1021/nn506960f

mechanical properties are mostly far away from that of human skin. Although cellulose/rubber composites have been reported in the literature,[16−19] none of them can closely replicate the mechanical properties of human skin. Even though cellulose/rubber composites also exhibit nonlinear property, they do not show the initial "toe" behavior, which is a critical characteristic of human skin, and their strains at failure are 4−10 times higher than that of skin. To the best of our knowledge, the design of materials to reproduce the mechanical properties of skin is still a great challenge.

Recently, researchers have developed a microstructure model to explain the nonlinear mechanical properties of skin (Supporting Information Figure S1).[20] According to this model, collagen fibers are uniformly dispersed in an elastin matrix and are chemically connected to elastin, with the elastin matrix also being cross-linked. The intermolecular cross-links of elastin play a crucial role in determining the characteristic mechanical properties of skin, in which collagen fibers are uniformly dispersed in the elastin matrix and are chemically connected by elastic elastin. Inspired by this model, we developed a strategy to prepare the synthetic materials with mechanical properties close to those of skin using two most abundant natural polymers, cellulose and polyisoprene (PI). First, it would be critical to combine two polymers with contrasting mechanical performances—one semirigid and strong and the other highly elastic—to mimic stiff collagen and elastic elastin in skin dermis, respectively. Second, the two polymers are chemically connected to allow for large, reversible deformation. Third, the two polymers microphase-separate into a multiphase nanocomposite in order to achieve the nonlinear mechanical properties of human skin. On the basis of these criteria, here we choose two abundant plant-based biopolymers, cellulose and natural rubber, which possess the desired contrasting mechanical properties, to design nanostructured elastomers mimicking the mechanical performance of human skin. Cellulose and collagen exhibit similar mechanical characteristics and are the two most abundant biopolymers serving mechanical functions in plant and animal tissues, respectively.[21,22] Therefore, we choose cellulose as a renewable and biocompatible biopolymer to mimic stiff collagen. Furthermore, we select a highly elastic biopolymer, polyisoprene (natural rubber), to mimic the elastic component of skin dermis, elastin. By covalently integrating these two natural biopolymers with opposite mechanical properties, we have synthesized two-phase nanostructured elastomers with the desired mechanical properties that closely mimic human skin. Importantly, the mechanical properties of the nanostructured elastomers can be tuned by adjusting cellulose content, providing the opportunity to synthesize materials that mimic the mechanical properties of different types of skins.

RESULTS AND DISCUSSION

The synthesis is illustrated in Figure 1. In the first step, brush polymers with a stiff cellulose backbone and elastic polyisoprene brushes are synthesized by the newly developed living/controlled radical polymerization method, activator regenerated by electron transfer atom transfer radical polymerization (ARGET ATRP).[23] Next, the brush polymers are cross-linked at the chain ends of polyisoprene brushes *via* ARGET ATRC (activator regenerated by electron transfer atom transfer radical coupling)[24] to form cross-linked brush polymers (CBPs) (Figure 1a,b). The amphiphilic CBPs self-assemble into a two-phase morphology consisting of stiff cellulose nanospheres and an elastic polyisoprene matrix, similar to the morphology observed for other brush polymer systems.[25] Finally, facilitated by cyclic tensile deformation, the cellulose nanospheres are converted to cellulose nanofibers, which are dispersed in the polyisoprene matrix, resembling the microstructure model of human skin (Figure 1c).

To demonstrate our nanostructured elastomers with the mechanical properties comparable to different types of human skin, we have prepared a series of CBPs with cellulose content varying from 4.3 to 20.6 wt % (**CBP1**−**5** samples in Table S1) by controlling the chain length of polyisoprene. Formation of the macroinitiator (Cell-BiB) was confirmed by Fourier transform infrared (FTIR) spectroscopy (Figure S2) and ^{1}H NMR spectra (Figure S3), and successful synthesis of CBPs was confirmed by solid-state CP/MAS ^{13}C NMR (Figure S4) and thermogravimetric analysis (TGA) (Figure S5). From the CP/MAS ^{13}C NMR spectrum of **CBP1**, we estimate that the propagating polyisoprene chains of about 28% were coupled *via* ARGET ATRC (see Supporting Information), indicating the formation of carbon−carbon bonds between the end groups of polyisoprene brushes.

The microphase separation behavior of the CBPs in the solid state was revealed by both dynamic mechanical analysis (DMA) and transmission electron microscopy (TEM) imaging. DMA curves during temperature sweeps for **CBP1**−**5** (Figure 2a,b) show two distinct glass transition temperatures (T_g), agreeing with a microphase-separated system (data summarized in Table S1, Supporting Information). The T_g values of the polyisoprene matrix phase range from −39 to −31 °C, which are slightly higher than that of natural rubber, presumably due to grafting to the rigid cellulose backbone and cross-linking. In contrast, the T_g values of the stiff cellulose backbone decrease from 184 to 64 °C with the increase of polyisoprene content. These results suggest partial phase mixing between the cellulose backbone and polyisoprene brushes. With the increase of cellulose content, the compatibility decreases and the T_g of polyisoprene decreases while the T_g of cellulose increases. In addition, the DMA storage modulus curves for **CBP1**−**5** (Figure 2b) show

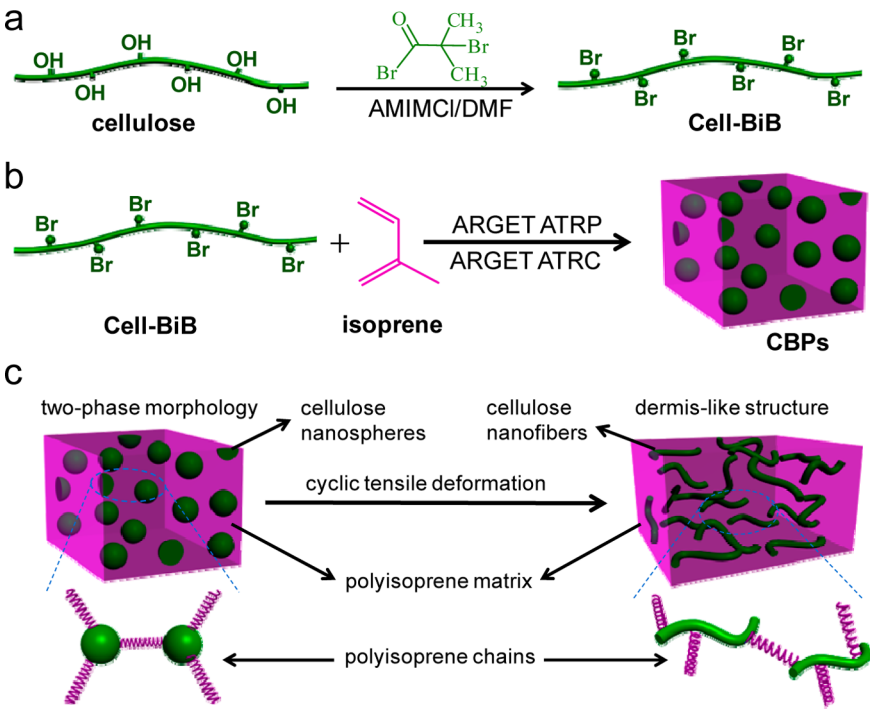

Figure 1. Design concept and synthesis of nanostructured elastomers mimicking the mechanical properties of human skin. (a) ATRP macroinitiator (Cell-BiB) was prepared using the previously reported method.[26] 1-Allyl-3-methylimidazolium chloride (AMIMCl) is a room temperature ionic liquid. (b) Cross-linked brush polymers were synthesized *via* ARGET ATRP and subsequent ARGET ATRC and self-assembled into two-phase morphology. (c) Two-phase morphology of CBPs can be reconfigured into that close to the skin microstructure model with cyclic tensile deformation.

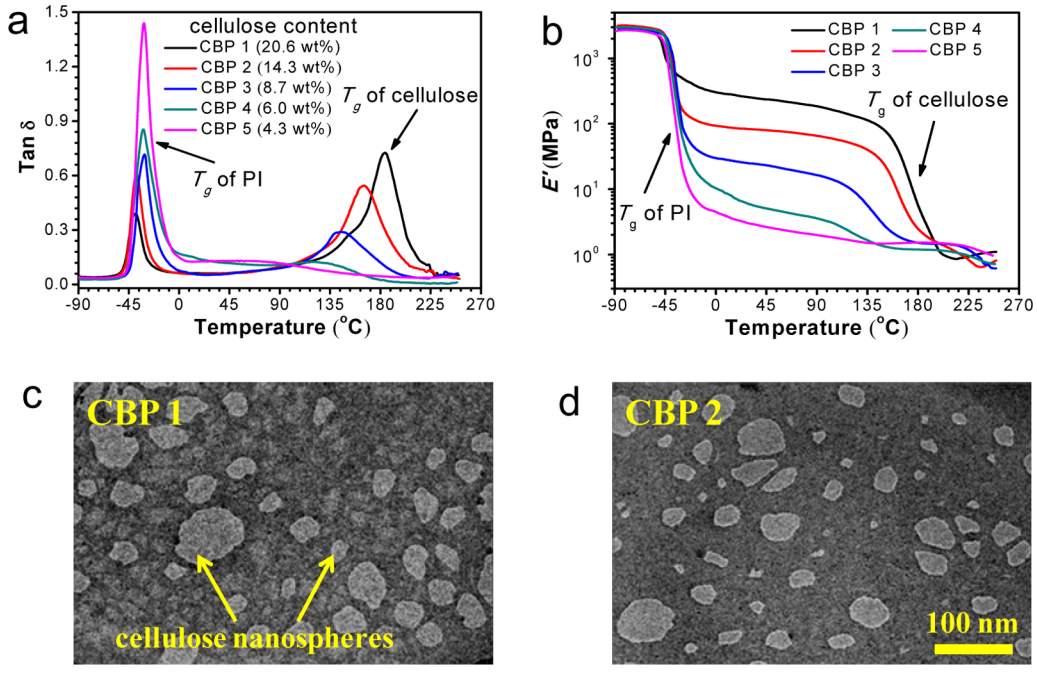

Figure 2. Characterization of microphase separation behavior of CBPs by DMA and TEM. DMA curves of loss tangent, tan δ (a), and storage modulus, E' (b), *versus* temperature for CBP1−5 samples, illustrating two distinct glass transition temperatures (T_g). TEM micrographs for CBP1 (c) and CBP2 (d), showing the two-phase morphology. Polyisoprene matrix phase was selectively stained with OsO_4. The scale bar in (d) represents 100 nm and is applied to (c), as well.

increased mechanical strength with increasing cellulose content at the intermediate temperature range relevant to practical applications. Besides thermal mechanical analysis, the two-phase morphologies of CBPs were also confirmed by TEM imaging. Figure 2c,d shows the typical TEM micrographs for **CBP1** and

CBP2, respectively, in which cellulose nanodomains with diameters less than 100 nm are dispersed in the polyisoprene continuous matrix phase.

Next, the synthesized CBPs were processed and post-treated in order to reproduce the microstructure model of human skin and mimic the mechanical performance of human skin. As shown by the TEM images (Figure 2c,d), the solid-state morphology of the as-made CBP samples shows cellulose nanodomains dispersed in the polyisoprene matrix, which is different from the skin microstructure model.[1] Accordingly, the mechanical properties of the as-made CBP samples measured by uniaxial tensile tests at room temperature do not follow that of human skin, as indicated by the stress−strain curve for **CBP1** during monotonic tensile deformation (Figure 3a, black line). Collagen in human skin dermis exists in nanofibers formed by protein self-assembly through polar and nonpolar interactions. A recent work demonstrated that repeated large-strain loading could lead to the persistent lengthening of collagen fibers.[27] Similarly, the cellulose nanodomains in CBPs are also formed by polar and nonpolar interactions. We reasoned that repeated tensile loading should be able to convert the morphology of cellulose nanodomains to cellulose nanofibers. Therefore, we applied cyclic tensile deformation to CBPs to reconfigure their morphology to that similar to the skin microstructure model. The stress−strain curve during cyclic tensile deformation for **CBP1** (Figure 3a, blue curve) shows large hysteresis in each cycle, with the upper envelope of the cyclic tensile deformation curve following closely the monotonic stress−strain curve (Figure 3a, black line), agreeing with the reported Mullins effect.[28] After the cyclic tensile deformation, the monotonic stress−strain curve of **CBP1** (Figure 3b) shows characteristic nonlinear elastic behavior resembling human skin. While soft at low strain, the stiffness of the treated sample rises gradually with increasing strain and finally increases linearly before failure.

Real-time synchrotron small-angle X-ray scattering (SAXS) and wide-angle X-ray diffraction (WAXD) analyses as well as TEM imaging revealed that the observed dramatic change of mechanical behavior for CBPs is due to reorganization of microstructure and change of morphology induced by cyclic tensile deformation treatment. The 2D SAXS patterns of **CBP1** during cyclic tensile deformation are shown in Figure 3a. Without any treatment, the 2D SAXS data of the as-made **CBP1** show a completely isotropic pattern at 0% strain, agreeing with the isotropic cellulose nanosphere morphology observed by TEM imaging (inset of Figure 3a). With an applied strain (120%), a scattering streak on the meridian appears, indicating plastic deformation and orientation of the rigid cellulose nanospheres. Figure S6a shows the true stress *versus* total true strain curve for **CBP1** during the cyclic deformation series in Figure 3a. From these curves, the plastic true strain, $\mathscr{E}_P$ (remaining strain at zero load), and elastic true strain, $\mathscr{E}_E$ (recovered strain after unloading), can be extracted. As proposed by Strobl and co-workers,[29] the maximal true strain, $\mathscr{E}$, in each cycle is the sum of a plastic component, $\mathscr{E}_P$, and an elastic component, $\mathscr{E}_E$. The elastic true strain, $\mathscr{E}_E$, and plastic true strain, $\mathscr{E}_P$, *versus* the maximal true strain, $\mathscr{E}$, at each cycle are shown in Figure S6b. It can be seen that the plastic true strain increases rapidly at small deformation and then levels off when the maximum true strain overcomes a critical point ($\mathscr{E} = 0.62$). The type of change can be explained by converting the crystalline lamellae into fibers by mechanical processing, as suggested by Strobl and co-workers.[29] This result demonstrates that the cellulose nanospheres in CBPs are converted into cellulose nanofibers, which become stabilized after the cyclic tensile deformation.

After cyclic tensile deformation treatment, a duck egg-like SAXS scattering streak on the meridian appears, further supporting that the cyclic tensile deformation treatment has indeed converted the cellulose nanospheres into nanofibers. The inset of Figure 3b clearly demonstrates the formation of cellulose nanofibers. This morphological change was also confirmed by 1D SAXS intensity profiles (Figure S7) and azimuthal intensity profiles (Figure S8) for **CBP1** during cyclic tensile deformation. The 2D WAXD patterns of **CBP1** confirm the absence of any crystalline structure during tensile deformations (this is further demonstrated by WAXD intensity profiles in Figure S9). From the azimuthal intensity profiles (Figure S10), it can be seen that the polyisoprene chains are orientated along the tensile direction during stretching and are disorientated during relaxing. Moreover, Figure S11 shows the nominal stress−nominal strain curves of **CBP1** during the first series of cyclic deformation (a), the second series of cyclic deformation (b), and the third series of cyclic deformation (c). It shows that the mechanical properties of CBPs become almost stable after the first series of cyclic deformation. Presumably, the microstructure of CBPs becomes stabilized after the first series of cyclic deformation so that mechanical properties of CBPs become repeatable if subsequent deformation does not exceed the previous deformation range. Based on the SAXS, WAXD, and TEM data, in the bottom of Figure 3a,b, we propose possible microstructure models corresponding to the various stages of deformation. Eventually, we obtained CBP samples exhibiting similar microstructure to the human skin microstructure model, with the stiff cellulose nanofibers (collagen fiber mimic) interwoven covalently with the elastic polyisoprene matrix (elastin mimic). Photos in Figure 3c visually show that **CBP1** (left side sample marked by A) becomes compliant after the cyclic tensile deformation (right side sample marked by B). We further propose the following molecular origin for the observed plastic deformation behavior. For the as-prepared CBPs,

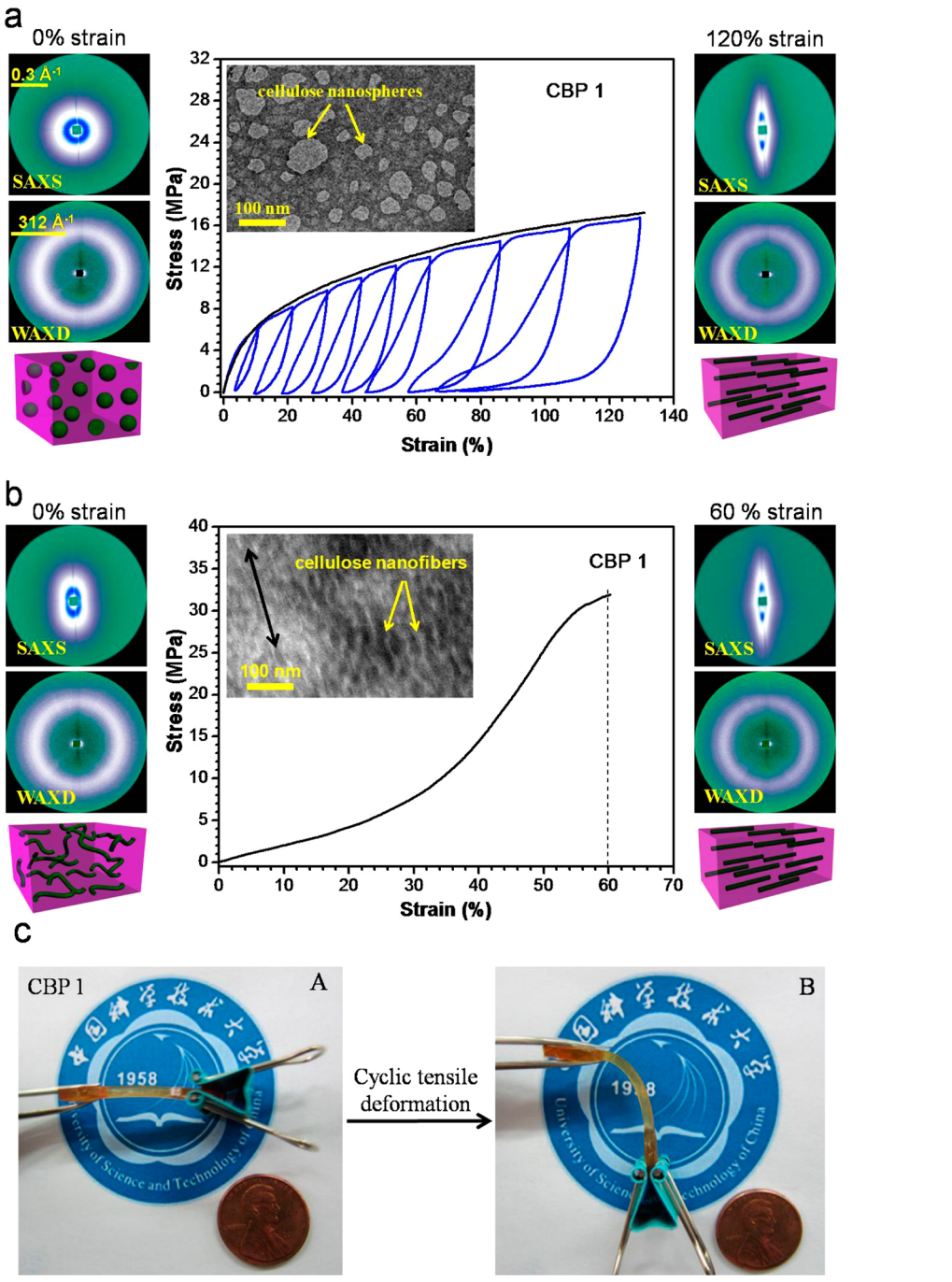

Figure 3. Cyclic tensile deformation to reconfigure the microstructure and reprogram the mechanical properties for CBPs. (a) Nominal stress–nominal strain curves of the CBP1 during monotonic tensile deformation (black line) and cyclic tensile deformation with maximum strains of 10, 20, and 30 and so on up to 130% (blue line). The strain rate was all fixed at 72%/min. Inset shows TEM image of CBP1 before cyclic tensile treatment, showing the nanosphere morphology of cellulose. (b) Monotonic nominal stress–nominal strain curve of CBP1 after cyclic tensile treatment. The dashed line indicates the strain at 60%. Inset shows TEM image of CBP1 after the treatment, which shows the formation of cellulose nanofibers. TEM samples were prepared by cryo-microtoming the treated CBP1 sample in parallel to the tensile direction. Polyisoprene matrix phase was selectively stained with OsO_4. The black arrow indicates the tensile direction. The corresponding real-time 2D SAXS patterns, 2D WAXD patterns (tensile direction is horizontal), and microstructural models for CBP1 during tensile deformation are displayed along with the stress–strain curves. (c) Photos of CBP1 before (A) and after (B) the cyclic tensile deformation. After the cyclic deformation treatment, the material became significantly more compliant so that the weight of a clamp could bend it.

hydrophilic cellulose backbones collapse into nanospheres uniformly dispersed in the polyisoprene matrix. The cellulose nanospheres are covalently connected by elastic polyisoprene chains during the polymerization and cross-linking. During the cyclic tensile deformation, the stress is transferred from polyisoprene chains to the covalently linked cellulose nanospheres. As the transferred stress is sufficiently high to overcome the physical

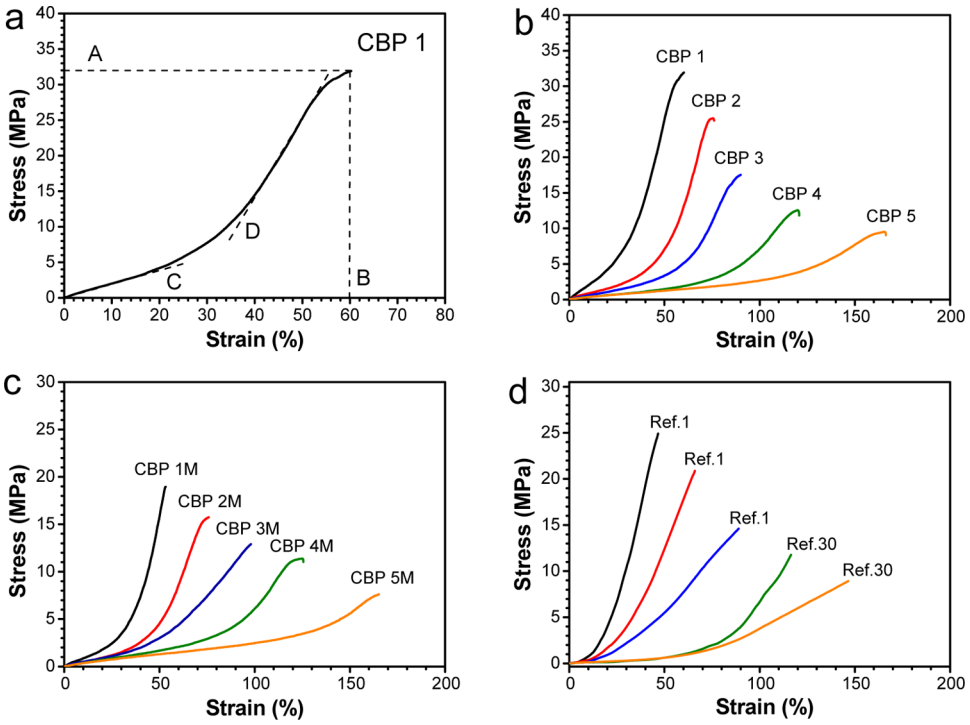

Figure 4. Tensile mechanical data for the bioinspired nanostructured elastomers and human skin samples. Monotonic nominal stress−nominal strain curve of CBP1 after cyclic tensile deformation treatment (a). The ultimate tensile strength is the maximum stress until failure of the specimen, A. The failure strain is the maximum strain obtained before failure, B. The initial elastic modulus is the slope of the curve at infinitesimal strains, C. The elastic modulus is defined as the slope of the linear portion of the curve, D. Monotonic nominal stress−nominal strain curves of CBP1−5 (b) and samples plasticized with 20 wt % mineral oil (CBP1−5M) (c) after cyclic tensile deformation treatment described in Figure 3a. Stress−strain responses of human skin samples reported in the literature (d).[1,30] The graph was digitized *via* GetData Graph Digitizer. The strain rate was all fixed at 72%/min.

interactions within cellulose nanospheres, cellulose nanospheres are converted into nanofibers and oriented along the tensile direction. After the tensile stress is released, the elastic polyisoprene chains recover quickly due to an entropic reason, which endows CBP samples an elastic behavior. However, there is no driving force to convert cellulose nanofibers back to nanospheres, resulting in the observed plastic deformation behavior. As reported by Weitz and co-workers, cyclic tensile deformation of collagen fibers can also lead to the plastic lengthening of collagen fibers.[27] The strain-induced cellulose nanofibers resemble collagen nanofibers in skin, and the combination of the stiff cellulose nanofibers and the elastic PI contributes to the close mimic of skin mechanical properties.

Crucially, the cellulose−polyisoprene nanostructured elastomers after cyclic tensile deformation treatment exhibit nonlinear elastic properties closely mimicking those of human skin. The tensile properties of **CBP1−5** after cyclic tensile deformation were thoroughly investigated and compared with those of human skin reported in the literature.[1,30] The nonlinear mechanical characteristics of **CBP1−5** (Figure 4b) are very similar to those of human skin (Figure 4d), as measured by stress−strain curves at the same strain rate of 72%/min. While relatively large deformation occurs at low stress, their stiffness rises gradually with increasing strain and finally increases linearly before failure. To the best of our knowledge, no synthetic materials reported previously show such nonlinear mechanical properties so closely mimicking those of human skin. In particular, the initial "toe" regions in nominal stress−nominal strain curves at early deformation observed in our materials have not been seen in other synthetic polymers reported so far. This "toe" behavior is a critical mechanical characteristic of human skin, which allows skin to be easily deformable at low strains and makes it feel soft. According to the solid-state CP/MAS ^{13}C NMR spectra (Figure S4), the propagating chain ends of 28% are coupled *via* ARGET ATRC, which means that a major fraction of the PI chains are not end-capped. These free chains may act as plasticizers, possibly helping lower the initial modulus, which is important to mimic the "toe" region of skin. Animal skins exist in the hydrate state, in which water molecules act as plasticizers to allow skin to have high strains with very low stress. In addition to replicating this unique "toe" behavior in the early deformation, our materials also show strong strain hardening in the late deformation stage similar to human skin. Finally, the maximal strains at the break of our materials are also very close to the values for human skin (50−150%). While some comparable properties may be found in other synthetic materials in the late

deformation stages, the ability to combine three key mechanical characteristics of skin (*i.e.*, the "toe" behavior in the early deformation, strong strain-hardening in the late deformation, and appropriate maximal strains at break) makes our materials very unique. The molecular origin for the unique mechanical properties of CBPs can be described as follows. At low strains, cellulose nanofibers are relaxed, and a soft elastic polyisoprene matrix is responsible for the initial mechanical properties of CBPs, which allows CBPs to have a "toe" region (low stress). After polyisoprene chains are straightened, stress is transferred to cellulose nanofibers and the modulus increases gradually with the alignment of cellulose nanofibers. Finally, the cellulose nanofibers are straightened, and CBPs show the stiff properties of aligned cellulose nanofibers.

In order to quantitatively compare the mechanical properties, a number of key characteristics from the stress–strain curves were identified as descriptive parameters and are illustrated in Figure 4a. These mechanical parameters for **CBP1**–**5** as well as human skin[1,30] reported in the literature are summarized in Table S2. The ultimate tensile strength for **CBP1**–**5** ranges from 34.3 ± 2.3 to 9.7 ± 0.5 MPa, the failure strain from 53 ± 7 to 166 ± 13%, the initial elastic modulus from 11.3 ± 0.6 to 2.1 ± 0.3 MPa, and the final elastic modulus from 142.5 ± 4.6 to 18.0 ± 1.2 MPa. It can be seen that most of our experimental results fall within the ranges of human skin found in the literature, except that the initial elastic moduli of **CBP1** (11.3 ± 0.6 MPs) and **CBP2** (6.6 ± 0.9 MPa) are slightly higher. Moreover, the elastic recovery values of **CBP1**–**5** (Figure S12) range from 72.8 to 97.2%, which are also comparable to that of human skin.[31] As human skin is hydrated with water, we added 20 wt % mineral oil to plasticize CBPs and modulate their mechanical properties. The stress–strain curves of the plasticized CBPs (**CBP1**–**5**) after cyclic tensile deformation treatment are shown in Figure 4c, and their mechanical properties are also summarized in Table S2. It is evident that the mechanical properties for the plasticized samples are even closer to those of human skin, with the initial elastic moduli of **CBP1**–**5M** all falling in the range for human skin. Furthermore, the stability of the mechanical properties of CBPs was investigated. Figure S13 shows the respective stress–strain curves for **CBP1**–**5** taken either immediately or 2 days after the cyclic tensile deformation. The shapes of the stress–strain curves for **CBP1**–**5** only change slightly after 2 days, demonstrating that the CBPs can maintain the desired skin-mimicking mechanical properties over time.

Skin surface wettability is an important factor of the skin protective function. Hence, we further investigated the wettability of CBPs and compared it with that of human skin. Water contact angle measurement is a conventional method to determine the relative wettability of materials.[32,33] Water contact angles for **CBP1**–**5** increase from 68.5 ± 1.3 to 82.3 ± 3.0° with the increase of polyisoprene content (Figure S14). Importantly, the wettability of CBP films is very close to that of human skin (water contact angle = 68 ± 8° for women, 86 ± 10° for girls, and 88 ± 6° for boys).[34–36] It also shows that the wettability of CBPs can be easily controlled to mimic different types of human skins by changing the chemical composition of the nanostructured elastomer materials.

CONCLUSIONS

Our results demonstrate a simple and effective strategy for designing new materials mimicking mechanical properties of human skin. By combining two naturally abundant biopolymers having contrasting mechanical properties, such as cellulose and natural rubber, we created a new type of nanostructured polymers with microstructures similar to that of the human skin microstructure model and mechanical properties comparable to those of human skin. The well-defined synthetic method allows for fine-tuning of the structures and mechanical properties of the designed nanostructured elastomers to mimic different type of skins. While the focus of the current study is mainly on exploring the new biomimetic design strategy, we believe that such materials can find various applications. For example, they may be used as skin mimics for robotics, prosthetics, and smart electronic devices. They may also be adopted for preparing artificial leathers that can more closely mimic human skin properties for comfortableness. With further development, we can apply the strategy to more biocompatible components to design a true skin substitute.

MATERIALS AND METHODS

Samples Synthesis. As shown in Scheme S1, preparation of the cellulose-based macroinitiator (Cell-BiB) was performed using previously published protocols.[26] As shown in Scheme S2, CBPs were synthesized *via* ARGET ATRP with *in situ* ARGET ATRC.[23] After being polymerized at 70 °C for 48 h, the resulting products were washed with THF to remove the catalyst and residual monomers and then dried under vacuum. The CBP samples were characterized by FTIR, ^{1}H NMR, solid-state CP/MAS ^{13}C NMR, and TGA measurements.

Tensile Tests. The cyclic tensile deformation and monotonic tensile tests of CBPs were carried out using a Linkam TST 350 tensile deformation test machine at room temperature. Each sample of CBPs was cut into a dog-bone-shaped specimen with a thickness of about 1 mm for the cyclic mechanical processing and mechanical property tests.

Morphology Characterizations. Low-temperature ultrathin sections (90 nm) were cut on a Leica EM Fc6 ultramicrotome, and the TEM observations were performed on a JEM-2010 conventional TEM operating at 120 kV. The polyisoprene matrix was stained by the vapor of 1% osmium tetraoxide (OsO_4) solution

before TEM observation. Synchrotron SAXS measurements were performed at SSRF, Shanghai, China. The wavelength of the X-ray radiation was 0.124 nm, and the sample-to-detector distance was 2417 mm. Synchrotron WAXD measurements were carried out at X-ray Diffraction and Scattering Beamline (U7B), National Synchrotron Radiation Laboratory (NSRL) in Hefei, China. The wavelength used was 0.154 nm. A detailed description of all applied techniques and characterization is given in the Supporting Information.

Conflict of Interest: The authors declare no competing financial interest.

Acknowledgment. Z.G.W. acknowledges the financial support from the National Science Foundation of China with Grant No. 51473155 and the National Basic Research Program of China with Grant No. 2012CB025901. Z.B.G. acknowledges the financial support from the U.S. Department of Energy, Division of Materials Sciences (DE-FG02-04ER46162), and National Science Foundation (DMR-1217651). The project was also funded by State Key Laboratory for Modification of Chemical Fibers and Polymer Materials, Dong Hua University, China.

Supporting Information Available: Detailed experimental section, Schemes S1 and S2, Tables S1 and S2, and Figures S1−S14. This material is available free of charge *via* the Internet at http://pubs.acs.org.

REFERENCES AND NOTES

1. Annaidh, A. N.; Bruyere, K.; Destrade, M.; Gilchrist, M. D.; Ottenio, M. Characterization of the Anisotropic Mechanical Properties of Excised Human Skin. *J. Mech. Behav. Biomed. Mater.* **2012**, *5*, 139–148.
2. Storm, C.; Pastore, J. J.; MacKintosh, F. C.; Lubensky, T. C.; Janmey, P. A. Nonlinear Elasticity in Biological Gels. *Nature* **2005**, *435*, 191–194.
3. Kushner, A. M.; Guan, Z. Modular Design in Natural and Biomimetic Soft Materials. *Angew. Chem., Int. Ed.* **2011**, *50*, 9026–9057.
4. Lv, S.; Dudek, D. M.; Cao, Y.; Balamurali, M. M.; Gosline, J.; Li, H. Designed Biomaterials To Mimic the Mechanical Properties of Muscles. *Nature* **2010**, *465*, 69–73.
5. Capadona, J. R.; Shanmuganathan, K.; Tyler, D. J.; Rowan, S. J.; Weder, C. Stimuli-Responsive Polymer Nanocomposites Inspired by the Sea Cucumber Dermis. *Science* **2008**, *319*, 1370–1374.
6. Jin, H. J.; Kaplan, D. L. Mechanism of Silk Processing in Insects and Spiders. *Nature* **2003**, *424*, 1057–1061.
7. Cranford, S. W.; Tarakanova, A.; Pugno, N. M.; Buehler, M. J. Nonlinear Material Behaviour of Spider Silk Yields Robust Webs. *Nature* **2012**, *482*, 72-U91.
8. Wilkes, G.; Brown, I.; Wildnauer, R. The Biomechanical Properties of Skin. *CRC Crit. Rev. Bioeng.* **1973**, *1*, 453.
9. Dunn, M. G.; Silver, F. H. Viscoelastic Behavior of Human Connective Tissues: Relative Contribution of Viscous and Elastic Components. *Connect. Tissue Res.* **1983**, *12*, 59–70.
10. Crichton, M. L.; Donose, B. C.; Chen, X. F.; Raphael, A. P.; Huang, H.; Kendall, M. A. F. The Viscoelastic, Hyperelastic and Scale Dependent Behaviour of Freshly Excised Individual Skin Layers. *Biomaterials* **2011**, *32*, 4670–4681.
11. Silver, F. H. The Importance of Collagen Fibers in Vertebrate Biology. *J. Eng. Fibers Fabr.* **2009**, *4*, 9–17.
12. Goldsmith, L. A. *Physiology, Biochemistry, and Molecular Biology of the Skin*, 2nd ed.; Oxford University Press: New York, 1991.
13. MacNeil, S. Progress and Opportunities for Tissue-Engineered Skin. *Nature* **2007**, *445*, 874–880.
14. Efimenko, K.; Rackaitis, M.; Manias, E.; Vaziri, A.; Mahadevan, L.; Genzer, J. Nested Self-Similar Wrinkling Patterns in Skins. *Nat. Mater.* **2005**, *4*, 293–297.
15. Takei, K.; Takahashi, T.; Ho, J. C.; Ko, H.; Gillies, A. G.; Leu, P. W.; Fearing, R. S.; Javey, A. Nanowire Active-Matrix Circuitry for Low-Voltage Macroscale Artificial Skin. *Nat. Mater.* **2010**, *9*, 821–826.
16. Flink, P.; Stenberg, B. Mechanical Properties of Natural Rubber/Grafted Cellulose Fibre Composites. *Br. Polym. J.* **1990**, *22*, 147–153.
17. Abdelmouleh, M.; Boufi, S.; Belgacem, M. N.; Dufresne, A. Short Natural-Fibre Reinforced Polyethylene and Natural Rubber Composites: Effect of Silane Coupling Agents and Fibres Loading. *Compos. Sci. Technol.* **2007**, *67*, 1627–1639.
18. Vieira, A.; Nunes, R. C.; Visconti, L. L. Mechanical Properties of NR/BR/Cellulose II Composites. *Polym. Bull.* **1996**, *36*, 759–766.
19. Coran, A.; Boustany, K.; Hamed, P. Short-Fiber-Rubber Composites: The Properties of Oriented Cellulose-Fiber-Elastomer Composites. *Rubber Chem. Technol.* **1974**, *47*, 396–410.
20. Delalleau, A.; Josse, G.; Lagarde, J. M.; Zahouani, H.; Bergheau, J. M. A Nonlinear Elastic Behavior To Identify the Mechanical Parameters of Human Skin *in Vivo*. *Skin Res. Technol.* **2008**, *14*, 152–164.
21. Fratzl, P. Cellulose and Collagen: From Fibres to Tissues. *Curr. Opin. Colloid Interface Sci.* **2003**, *8*, 32–39.
22. Mathew, A. P.; Oksman, K.; Pierron, D.; Harmad, M. F. Crosslinked Fibrous Composites Based on Cellulose Nanofibers and Collagen with *In Situ* pH Induced Fibrillation. *Cellulose* **2012**, *19*, 139–150.
23. Jakubowski, W.; Matyjaszewski, K. Activators Regenerated by Electron Transfer for Atom-Transfer Radical Polymerization of (Meth)Acrylates and Related Block Copolymers. *Angew. Chem., Int. Ed.* **2006**, *45*, 4482–4486.
24. Domingues, K. M.; Tillman, E. S. Radical−Radical Coupling of Polystyrene Chains Using AGET ATRC. *J. Polym. Sci., Part A: Polym. Chem.* **2010**, *48*, 5737–5745.
25. Chen, Y.; Kushner, A. M.; Williams, G. A.; Guan, Z. Multiphase Design of Autonomic Self-Healing Thermoplastic Elastomers. *Nat. Chem.* **2012**, *4*, 467–472.
26. Jiang, F.; Wang, Z. K.; Qao, Y.; Wang, Z. G.; Tang, C. B. A Novel Architecture toward Third-Generation Thermoplastic Elastomers by a Grafting Strategy. *Macromolecules* **2013**, *46*, 4772–4780.
27. Münster, S.; Jawerth, L. M.; Leslie, B. A.; Weitz, J. I.; Fabry, B.; Weitz, D. A. Strain History Dependence of the Nonlinear Stress Response of Fibrin and Collagen Networks. *Proc. Natl. Acad. Sci. U.S.A.* **2013**, *110*, 12197–12202.
28. Mullins, L. Softening of Rubber by Deformation. *Rubber Chem. Technol.* **1969**, *42*, 339–362.
29. Men, Y.; Rieger, J.; Strobl, G. Role of the Entangled Amorphous Network in Tensile Deformation of Semicrystalline Polymers. *Phys. Rev. Lett.* **2003**, *91*, 095502.
30. Jansen, L.; Rottier, P. Some Mechanical Properties of Human Abdominal Skin Measured on Excised Strips. *Dermatology* **1958**, *117*, 65–83.
31. Gerhardt, L. C.; Lenz, A.; Spencer, N. D.; Muenzer, T.; Derler, S. Skin-Textile Friction and Skin Elasticity in Young and Aged Persons. *Skin Res. Technol.* **2009**, *15*, 288–298.
32. Xi, Z. Y.; Xu, Y. Y.; Zhu, L. P.; Wang, Y.; Zhu, B. K. A Facile Method of Surface Modification for Hydrophobic Polymer Membranes Based on the Adhesive Behavior of Poly(DOPA) and Poly(Dopamine). *J. Membr. Sci.* **2009**, *327*, 244–253.
33. Luo, J. Y.; Wu, C. M.; Wu, Y. H.; Xu, T. W. Diffusion Dialysis of Hydrochloride Acid at Different Temperatures Using PPO-SiO_2 Hybrid Anion Exchange Membranes. *J. Membr. Sci.* **2010**, *347*, 240–249.
34. Mavon, A.; Zahouani, H.; Redoules, D.; Agache, P.; Gall, Y.; Humbert, P. Sebum and Stratum Corneum Lipids Increase Human Skin Surface Free Energy As Determined from Contact Angle Measurements: A Study on Two Anatomical Sites. *Colloids Surf., B* **1997**, *8*, 147–155.
35. Pailler-Mattei, C.; Nicoli, S.; Pirot, E.; Vargiolu, R.; Zahouani, H. A New Approach To Describe the Skin Surface Physical Properties *in Vivo*. *Colloids Surf., B* **2009**, *68*, 200–206.
36. Ginn, M.; Noyes, C.; Jungermann, E. The Contact Angle of Water on Viable Human Skin. *J. Colloid Interface Sci.* **1968**, *26*, 146–151.